ON THE SHAPE OF LIQUID METAL DROPLETS IN ELECTROMAGNETIC LEVITATION EXPERIMENTS

E. Schwartz*, S. Sauerland**, J. Szekely*, I. Egry**

* Department of Materials Science and Engineering, Massachusetts Institute of Technology, Cambridge, MA 02139, USA

** Institute for Space Simulation, German Aerospace Research Establishment, DLR, 5000 Koeln 90, Germany

Abstract

We present calculations and measurements on the shape of liquid metal droplets in electromagnetic levitation experiments. A normal stress balance model was developed to predict the shapes of liquid metal droplets that will be obtained in a microgravity experiment to measure the viscosity and surface tension of undercooled metals. This model was tested by calculating the droplet shapes in containerless experiments conducted to determine the surface tension of liquid metals. Inconsistencies associated with the results of a previous paper are elucidated. The computational results of the mathematical model are compared with the results of ground-based experiments for two different metals. The importance of the ratio of electromagnetic skin depth-to-droplet radius to the accuracy of the mathematical model is discussed. A planned alternate approach to modeling the shape by consideration of the entire droplet rather than only the surface is presented. As an example of an application, the influence of the shape on the splitting of the surface oscillation modes of levitated liquid metal droplets is discussed.

Introduction

In recent years electromagnetic levitation has become both a widely-used experimental technique and an important part of the field of materials processing. Levitation of liquid metal droplets provides a clean, containerless environment that makes it possible to perform high-precision experiments and process reactive metals with high melting points.

Electromagnetic levitation provides the opportunity to perform experiments on undercooled liquid metals in such areas as the study of nucleation and recalescence and measurement of thermophysical properties such as heat capacity, surface tension, and viscosity. The behavior of undercooled melts has both fundamental and practical interest. Undercooled melts are now being processed in technologies such as near net shape casting and rapid solidification. This requires increased knowledge about the melt-solid phase transition and the temperature dependence of thermophysical properties [1].

Containerless Processing: Techniques and Applications
Edited by W. Hofmeister
The Minerals, Metals & Materials Society, 1993

For most thermophysical property measurements, the shape of the liquid metal droplet must be known for the interpretation of the results. This is one reason why it is desirable to have the ability to predict these shapes for a given coil geometry, applied current, and sample material. Development of a mathematical model of the shape of liquid metal droplets in electromagnetic levitation experiments also makes it possible to optimize the experiment parameters in order to achieve desired sample shapes and positions.

The surface tension and viscosity of selected undercooled metals will be measured in a microgravity experiment during the NASA IML-2 mission, which is scheduled to fly in 1994. The TEMPUS system is the electromagnetic levitation device that will be used to position and excite oscillations in the liquid metal droplets. A schematic sketch of the TEMPUS system is provided in Figure 1. Prediction of the sample shapes that will occur in the flight experiment will enable the precise measurement of thermophysical properties.

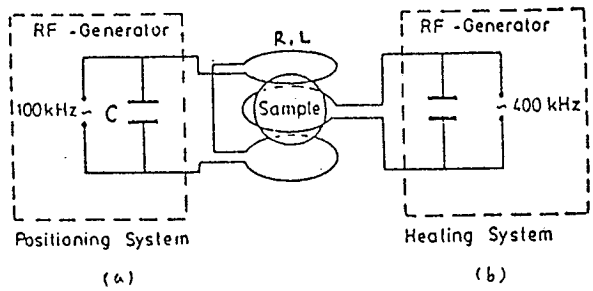

Figure 1: Schematic diagram of TEMPUS system with separate (a) positioning and (b) heating coil systems.

This work is intended to update the results presented during the MHD Symposium at the 1992 TMS Annual Meeting [2]. In that paper results were presented suggesting the agreement between the predicted and measured shape of a levitated metal droplet. It has since been discovered that the agreement was achieved as a result of self-canceling errors in measurement and calculation. The errors present in the previous work are

addressed, and a new comparison of experimentally-determined and calculated shapes for two different metals is presented. This paper is designed to be a report on our progress in modeling the shape of levitated metal droplets, and discusses how we are addressing the complex issues involved.

Formulation and Computational Methodology

The two major computational tasks associated with modeling the equilibrium shape of an electromagnetically-levitated molten metal droplet are calculation of the magnetic field distribution in the droplet and calculation of the shape, which is determined by equilibrium of the component of stress normal to the surface of the droplet.

(i) Electromagnetic calculations

The magnetic field distribution in the levitated droplet is calculated using the method of mutual inductances presented by, among others, El-Kaddah and Szekely [3] and Zong et al. [4]. The axisymmetric levitated droplet is discretized into a set of annular electrical circuits through which induced current flows. Once the induced current distribution is calculated, the distribution of magnetic flux density can be calculated by taking the curl of the distribution of vector potential, or by using the Biot-Savart law. Use of the Biot-Savart Law is preferable because it utilizes numerical integration as opposed to numerical differentiation, which is prone to numerical errors. The Biot-Savart Law was used in the calculations that provided the results presented here. This represents an improvement over the previous model.

The discretization of the droplet domain and the shape of the cross section of the annular circuits can be seen in Figure 2. Also visible is the exponential distribution of grid points used to better represent the distribution of magnetic flux density, which decays exponentially from the magnitude at the surface with distance into the droplet. In this paper an important modification to the calculation of mutual inductances between each pair of annular circuit elements, which have an approximately rectangular cross section, is made.

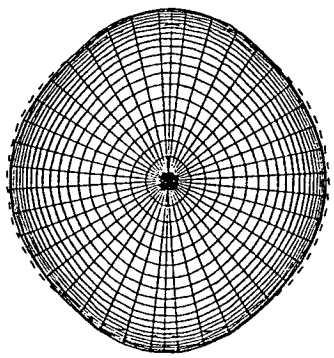

Figure 2: Discretization of droplet domain, showing exponential grid point distribution and rectangular cross section of annular circuit elements.

Maxwell's formula for the mutual inductance between two coaxial wires assumes that the cross section of the wires is circular. Following Dudley and Burke [5] and Burke et al. [6], Lyle's method is used to replace the approximately rectangular circuit elements with two representative locations at which Maxwell's formula can be applied. The mutual inductance between a pair of rectangular circuit elements is then found by averaging the mutual inductances calculated with Maxwell's formula at these locations. The method was further adapted to account for the fact that the sides of the approximately rectangular cross sections were not always oriented parallel and perpendicular to the axis of symmetry, as can be seen in Figure 2. Furthermore, a formula from Burke et al. [6] is used to calculate the self-inductance of the annular circuit elements of approximately rectangular cross section.

(ii) Free surface shape calculations

There are two self-consistent methods by which the equilibrium shape of an electromagnetically-levitated molten metal droplet has been modeled. The equilibrium shape is calculated either by balancing the normal stresses at each point on the free surface (known as the local method) [2,7-9] or by minimizing the total energy of the system (global method) [8,10-15].

Both models assume that the electromagnetic skin depth

$$\delta = \sqrt{\frac{2}{\omega \mu_o \sigma}} = \sqrt{\frac{1}{\pi \nu \mu_o \sigma}} \qquad (1)$$

which characterizes the distance into the droplet of electrical conductivity σ that the external magnetic field of frequency ν can penetrate, is much smaller than the radius of the droplet, allowing the conclusion that internal fluid flow does not influence the free surface shape and can be ignored. In the case of very thin skin depth, the molten metal droplet behaves like a perfect conductor into which the magnetic field would not penetrate and in which no fluid flow would be driven.

In other words, it is assumed either that the flow is inviscid ($\mu = 0$) or non-existent ($\vec{u} = \vec{0}$). Either one of these assumptions is sufficient to eliminate the normal viscous stress from the free surface boundary condition.

Differences between the two modeling approaches largely concern the rate of convergence to the equilibrium shape. According to Bhamidipati and El-Kaddah [16], in the energy minimization technique, the displacement of the melt free surface from non-equilibrium to equilibrium shape is precisely defined in terms of the derivative of the variational statement of the energy functional of the system, thus ensuring rapid convergence. The local stress balance method, though simpler to implement, relies on arbitrary choice of displacement, and requires more iterations to obtain a converged solution.

(a) Normal stress balance method(Local method)

This method is the technique most frequently used in developing mathematical models of electromagnetic shaping operations, such as the shape of the meniscus in electromagnetic casting [16-22].

At equilibrium the net normal stress at all points along the free surface is zero. The normal component of the stress balance is given by

$$(p_H - p_a) + \rho g(z_{top} - z) + T_{mm} - \gamma\left(\frac{1}{R_1} + \frac{1}{R_2}\right) = 0 \qquad (2)$$

Before considering the shape determination algorithm, it is useful to consider how the various physical phenomena contribute to the normal stress balance by examining the terms in Equation (2).

(1) Hydrostatic pressure

The first term represents the difference between the hydrostatic pressure p_H, which is uniform throughout the entire fluid, and the atmospheric pressure.

(2) Gravitational head

The second term is the gravitational head, referenced to the top of the droplet, thereby defined to be positive everywhere. The contribution to the pressure of the gravitational head at any point in the droplet depends on the pressure at the top of the sample, the depth of the point, and the specific weight (ρg) of the fluid [23]. The gravitational head at any point in the droplet is referenced to the pressure at the top of the droplet by taking the contribution of gravitational head to the pressure at that point to be zero.

Pressure always acts from the liquid in the direction normal to a surface [23], therefore, the hydrostatic pressure and the gravitational head exert a normal force per unit area on the surface in the outward direction.

(3) Magnetic pressure

The third term is the normal stress component of the Maxwell stress tensor, representing the force per unit area exerted by the external magnetic field on the surface. This is commonly called the magnetic pressure, and only depends on the tangential component of the magnetic field because there is no component of magnetic field normal to the surface in the small skin depth approximation. In terms of the magnetic flux density, the magnetic pressure is [4]

$$p_m = T_{mm} = \frac{-B_t^2}{2\mu_o} \qquad (3)$$

where B_t is the temporal average of the tangential component of the time-dependent magnetic flux density.

(4) Surface tension surface force density

The final term in the normal stress balance represents the surface force density due to surface tension [17]. The surface tension of the droplet is γ, and the two principal radii of curvature of the surface R_1 and R_2 are defined as positive for the outward-bulging surface [24]. The formulas used to calculate the principal radii of curvature in axisymmetric spherical coordinates are presented in [2]. The effect of surface tension at a given point is directed inward and normal to the surface.

The hydrostatic pressure and gravitational head contribute a normal force per unit area outward from the surface, while the magnetic pressure and surface tension surface force density exert an inward normal force per unit area.

The equilibrium free surface shape is calculated as follows [2,4]:

(i) The magnetic flux density distribution inside the droplet is calculated using the method of mutual inductances and the Biot-Savart law, as described above, for the initial shape, a sphere.

(ii) The gravitational head, magnetic pressure, and surface tension surface force density are calculated at a finite number of points on the surface. From these contributions, a stress imbalance at each of these points is calculated. Based on the algebraic sign conventions used above, this value will be negative at all points on the surface. (Note that this value will vary along the surface until the free surface shape which satisfies the equilibrium condition, Equation. (2), is found.)

(iii) The surface-area weighted average stress imbalance for the surface is then calculated, after which the difference from this weighted average at each point on the surface is calculated. The difference will be positive at some points and negative at others. If the value is negative, this indicates that the magnitude of the stress imbalance at that point is greater than the magnitude of the weighted average stress imbalance, and the point should be moved inward (toward the center of the droplet).

(iv) Each point on the surface is moved in the radial direction along a line of constant angle (sometimes called a spine) by an amount proportional to the difference between the stress imbalance and the surface-area weighted average at that point. This ensures that the volume of the droplet will be conserved. A new shape is determined by these displacements of the surface.

(v) The sum of the squares of the differences between the stress imbalance and the weighted average at all points along the surface is calculated as an indicator of how much the current free surface shape deviates from the equilibrium shape. A sum of squares is used to prevent positive and negative values from canceling each other and falsely suggesting that equilibrium has been

achieved. When this sum of squares is less than a critical value, the equilibrium shape has been found to within a given tolerance. If this condition is not satisfied, then the procedure is repeated.

The results presented in this paper were obtained using the normal stress balance method.

(b) Energy minimization (Global method)

The equilibrium shape of the free surface, resulting from a balance among magnetic pressure, surface tension, and gravity forces, is governed by the equation [11]

$$\frac{B^2}{2\mu_o} + \gamma K + \rho g z = const. \qquad (4)$$

where B is the root-mean-square magnitude of the local magnetic field, and K is the sum of the principal radii of curvature of the droplet.

An energy functional for the variational technique is defined which represents the total energy of the system. For droplet domain Ω and free surface boundary $\partial\Omega$, the energy functional is [11]

$$\phi(\Omega) = -\iiint_{R^3} \frac{B^2}{2\mu_o} dv + \iint_{\partial\Omega} \gamma ds + \iiint_{\Omega} \rho g z dv \qquad (5)$$

In order to minimize the total energy with respect to the constant volume constraint on the droplet, a new functional using the Lagrange multiplier λ is defined. It is given by [12]

$$\psi(\Omega) = \phi(\Omega) - \lambda \iiint_{\Omega} dv \qquad (6)$$

where λ is expressed as [12]

$$\lambda = \frac{\iint_{\partial\Omega} \left(\frac{B^2}{2\mu_o} + \gamma K + \rho g z \right) ds}{\iint_{\partial\Omega} ds} \qquad (7)$$

Using the global method, the equilibrium free surface shape is calculated as follows [8]:

(i) The magnetic flux density distribution at the surface of the droplet is calculated by considering elements at the surface and the region outside the droplet, which is made possible by the assumption of small or zero skin depth. The initial shape is a sphere.

(ii) The magnetic energy, surface energy, and gravitational energy are calculated along $\partial\Omega$.

(iii) The Lagrange multiplier for the surface is calculated using Equation (7). Note that λ is the surface-area weighted average free energy for the surface, and is completely analogous to the surface-area weighted stress imbalance calculated in step (iii) of the normal stress balance method above.

(iv) The displacement of the surface effected reduces $\psi(\Omega)$ with magnitude determined by an adjustable coefficient that permits rapid convergence.

(v) If the derivative of the functional with respect to the domain, $\partial\psi / \partial\Omega$, is not sufficiently small, then the procedure is repeated.

Experimental Work

The experiments were performed on pure nickel and copper droplets (Johnson Matthey, 99.99%) with mass of approximately 1 g. A detailed description of the levitation facility at DLR is given in [25]. A conical coil arrangement that provided stable levitation of the droplets was used. A sketch of the coil geometry, as well as the strength of the external magnetic field and magnetic field gradient on the symmetry axis of the coils for a peak applied current of I_o = 405 A, which was used in the case of the nickel sample, is shown in Figure 3.

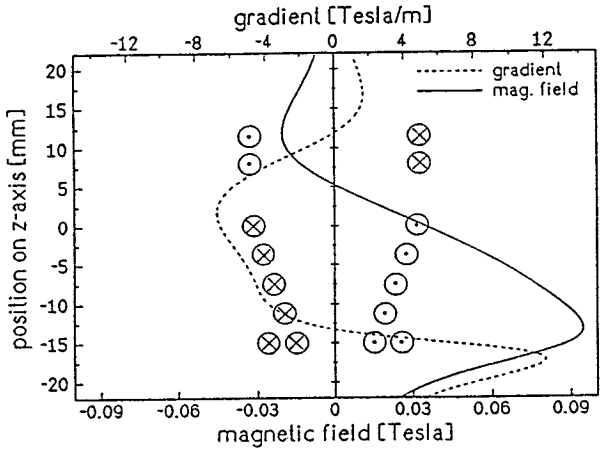

Figure 3: Conical coil arrangement with field strength for a peak applied current of I_o=405 A.

The RF-generator was operated at a frequency of 333 kHz. The peak applied coil currents were 405 A, in the case of nickel, and 310 A, in the case of copper. The samples were convectively cooled by He gas. Non-contact temperature measurement was performed with a standard two-color ratio pyrometer.

Experiments with nickel and copper droplets were performed in the same way. The droplet was levitated with the coil current given above. During levitation, the translational oscillation frequencies and the surface oscillation frequencies were measured using a method explained in [26] and [27]. The samples were then rapidly solidified by cooling with He gas. The volume change upon solidification was assumed to be isotropic and,

therefore, shape-preserving. Figure 4 shows a picture of a sample processed in this way. Next to this is a shape measured from a projection onto a grid and a fit of spherical harmonics

$$R(\psi) = R_o\left(1+\sum_{l=1}^{n}\varepsilon_l Y_l^0(\psi)\right) \qquad (8)$$

at the contour is shown to give an image of the distortion from spherical shape.

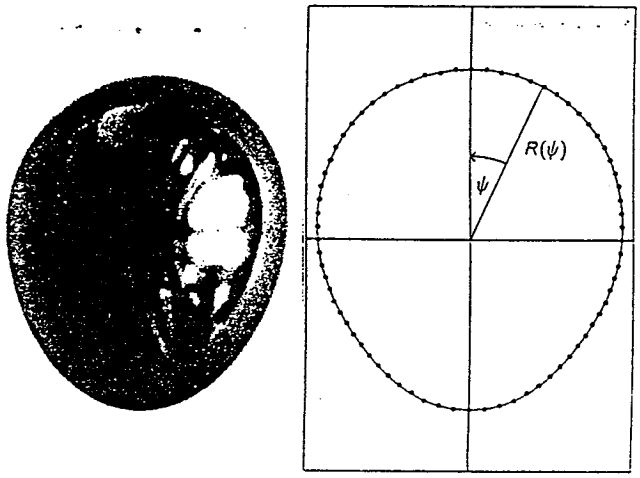

Figure 4: Fit of spherical harmonics to experimental shape.

In order to eliminate the effect of "frozen-in" oscillations on the shape of the rapidly-solidified droplet, the mean values of measurements made on many levitated and solidified droplets were used to determine the experimentally-determined equilibrium shape. The measured coefficients of the spherical harmonics ε_l (with errors $\Delta\varepsilon_l$) are listed in Table 1.

l	ε_l	$\Delta\varepsilon_l$
0	3.545	0.007
1	0.088	0.006
2	0.141	0.006
3	-0.048	0.005
4	0.015	0.006
5	-0.004	0.006

Table 1: Expansion coefficients of R(ψ).

An important application of the knowledge of the distortion of a levitated droplet is the influence on the surface oscillation modes of levitated droplets.

In the oscillating drop technique, the frequencies of the surface oscillations are used to determine the surface tension of liquid metals. Due to gravity and a lack of spherical symmetry, the fundamental oscillation mode is split into a number of modes, each with its own frequency. The measurements then yield spectra with multiple peaks, with a maximum of five. Cummings et al. [28] and Suryanarayana et al. [29] have recently calculated the effect of distortion of the sample from a spherical shape on individual frequencies. According to Cummings [28] the frequencies of the five modes are expressed in terms of the Rayleigh frequency $\nu_R = \sqrt{8\gamma/3\pi m}$ as

$$\begin{aligned}
\nu_{2,0} &= \nu_R(1-0.6758\varepsilon_2-2.1760\varepsilon_4)\\
\nu_{2,\pm1} &= \nu_R(1-0.3379\varepsilon_2+1.4507\varepsilon_4)\\
\nu_{2,\pm2} &= \nu_R(1+0.6758\varepsilon_2-0.3627\varepsilon_4)
\end{aligned} \qquad (9)$$

with the coefficients ε_l defined in Equation (8). Both authors indicated that assignment of the modes is essential to obtaining precise results in the measurement of surface tension by this technique.

These results have been experimentally verified by Sauerland et al. [27] using digital image processing methods. Table 2 shows the good agreement between the splitting of the modes for the nickel sample in Figure 4 as predicted by Equation (9) and the measured oscillation frequencies.

	ν_0/ν_R	ν_1/ν_R	ν_2/ν_R
calculated	0.914	0.974	1.089
measured	0.928	0.979	1.057

Table 2: Comparison of frequency splitting.

To summarize, there is significant interest in having a tool to predict the deformation of droplets in levitation experiments because it would allow them to apply the theories of Cummings et al. and Suryanarayana et al. directly. This would enable prediction of the mode splitting that would result, facilitating assignment of oscillation modes and increasing the precision of surface tension measurements.

Computed Results

The equilibrium free surface shapes of molten liquid copper and nickel droplets were calculated using the input parameters listed in Table 3, which correspond to the experimental conditions

Parameter	Cu	Ni
Applied current (A)	310	405
Frequency (kHz)	333	333
Radius of sphere (mm)	2.982	3.11
Conductivity $(\Omega m)^{-1}$	5×10^6	1.205×10^6
Density (kg/m^3)	8106	8080
Surface tension (N/m)	1.45	1.82

Table 3: Input parameters used for equilibrium free surface shape calculations.

described above. Plots of the experimentally-determined shape, indicated by a solid line, and the calculated shape, indicated by a dashed line, are provided for copper and nickel in Figures 5 and 6, respectively. In each figure the dotted line represents the shape of a sphere of equal volume.

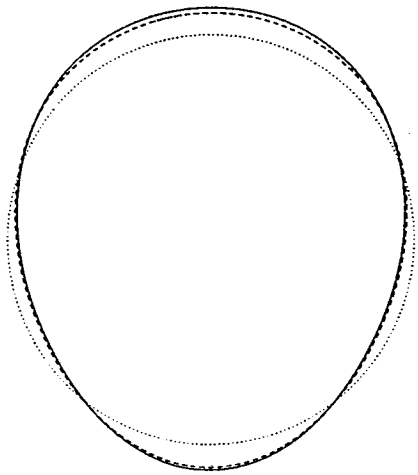

Figure 5: Comparison of results for Cu droplet.
..... Spherical shape
— Experimentally-determined shape
--- Calculated deformed shape

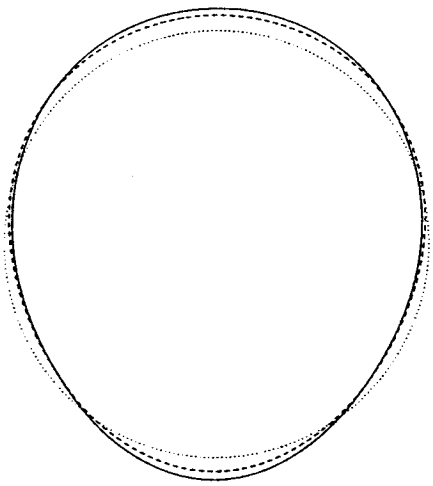

Figure 6: Comparison of results for Ni droplet.
..... Spherical shape
— Experimentally-determined shape
--- Calculated deformed shape

From the figures it can be seen that the calculated shapes agree quite well with the experimentally-determined shapes, but it is important to realize that the visual comparison is quite flattering because the deformation of the droplet is relatively small. In each case the calculated shape correctly depicts the teardrop shape produced due to gravity in samples levitated under earthbound conditions.

Discussion

The ability to predict, through mathematical modeling, the equilibrium free surface shape of electromagnetically-levitated droplets is important to the performance of surface tension measurements by the oscillating drop technique. This is quite a substantial undertaking due to the coupling of many complex phenomena, principally electromagnetic phenomena, free surface phenomena, and internal fluid flow.

In the normal stress balance model presented here, the small skin depth approximation was used in order to calculate the free surface shape of the sample by considering only the surface and neglecting the interior of the droplet. The ideal case for this model would then involve a sample of infinite conductivity (zero skin depth). However, in the cases of the copper and nickel droplets considered here, the skin depth is 13.08% of the radius for the copper droplet, and 25.55% of the radius for the nickel droplet. Both of these thereby constitute a deviation from the ideal case for this model.

This helps to interpret the results shown in Figures 5 and 6. In both cases, the calculated shape is less deformed than the experimentally-determined shape. The reason for this is that, since the sample has finite conductivity (and a nonzero skin depth to droplet radius ratio), there is some penetration of the field into the interior of the droplet. As a result, the magnitude of the magnetic pressure, calculated from the magnitude of magnetic flux density at the surface provides a lower bound estimate of the deforming effect of the magnetic field. A consideration of the skin depth-to-radius ratios for the two cases predicts the result that the calculated shape matches the experimental shape better in the case of copper than in the case of nickel.

Figures 5 and 6 show that the normal stress balance model provides a good estimate of the equilibrium free surface shape of levitated metal droplets. In order to achieve even better agreement, the computed results herein suggest that, when the ratio of skin depth to sample radius is not negligible, the interior of the sample must be considered. This finding is also useful for modeling the shapes of electromagnetically-shaped liquid metals in general. In order to model the free surface shape of a large pool of molten metal subjected to electromagnetic forces, consideration of the surface is sufficient, however, in cases where the sample dimensions are small, as is often the case with meniscus control, the interior of the droplet must be considered.

Planned Approach

Solution of the Navier-Stokes equations with an electromagnetic force fluid flow source term and a free surface boundary condition allows the effect of the electromagnetic force distribution on the interior of the droplet to be considered.

The Navier-Stokes equations take the following form:

$$\frac{\partial \vec{u}}{\partial t} + \vec{u} \cdot \vec{\nabla} \vec{u} = -\frac{1}{\rho} \vec{\nabla} p + \frac{1}{\rho} \vec{\nabla} \cdot \left(\mu \vec{\nabla} \vec{u} \right) + \vec{g} + \vec{F}_{EM} \qquad (10)$$

where $\vec{u}$ is the velocity vector field, which represents the internal flow in the droplet, and μ is the viscosity of the fluid.

The distribution of electromagnetic force per unit mass is expressed as

$$\vec{F}_{EM} = \vec{J} \times \vec{B} \qquad (11)$$

where $\vec{J}$ is the induced current density and $\vec{B}$ is the magnetic flux density. This electromagnetic force distribution is calculated as described above, and supplied as a source of fluid flow to a computational fluid mechanics package such as FIDAP or PHOENICS, which would numerically solve Equation (10), subject to the free surface boundary condition for axisymmetric geometries. This is given by a balance of normal components of stress as

$$(p - p_a) = \gamma \left(\frac{1}{R_1} + \frac{1}{R_2} \right) + 2\mu \frac{\partial u_n}{\partial n} \qquad (12)$$

where the difference between the fluid pressure and the atmospheric pressure p_a is equal to the sum of the surface tension surface force density and the normal component of viscous stress at the free surface. The coordinate n represents the curvilinear coordinate normal to the surface. In static fluids, Equation (12) reduces to Laplace's formula.

An order-of-magnitude analysis of the terms in the free surface boundary condition, Equation (12), indicates that the normal component of the viscous stress is roughly three orders of magnitude smaller than the surface tension surface force density. This suggests that the internal fluid flow itself does not govern the shape of the free surface. The salient point to make about the calculation method involving solution of the Navier-Stokes equations is that it allows for a more accurate representation of the electromagnetic phenomena in the droplet.

Fukumoto et al. [30] have used this approach to predict the meniscus shape in an electromagnetic caster. It was found that the results of simulations in which flow was considered and in which flow was neglected were similar at higher frequencies. This must be due to the existence of smaller skin depth at higher frequencies, which translates to less internal fluid flow, as discussed above.

This approach constitutes a considerable computational undertaking because the transient free surface shape and the electromagnetic force distribution simultaneously influence each other, requiring that the Navier-Stokes equations and the equations governing the electromagnetic phenomena be solved at each time step. It is important to note, however, that the equations governing the fluid flow and electromagnetic phenomena are decoupled by the assumption that the internal fluid flow in the droplet does not affect the magnetic field distribution. This allows the electromagnetic force distribution to be calculated using the free surface shape determined for the previous time step and subsequently supplied to the Navier-Stokes equations as a source term in order to calculate the new internal fluid flow field and free surface shape.

Calculation of the free surface shape by solution of the Navier-Stokes equations is further complicated by the fact that the internal fluid flow in the droplets levitated in ground-based experiments is turbulent. Turbulent flow is particularly difficult to model in this system because the entire domain is bounded by a free surface.

To address the problem of non-negligible skin depth-to-radius ratio in these systems, we have begun a computational effort to couple the electromagnetics code that we have developed with the finite-element fluid flow package FIDAP so that the magnetic field distribution can be re-calculated at each time step as the free surface shape of the droplet changes.

Acknowledgements

The authors acknowledge the financial support provided by the National Aeronautic and Space Administration under contract number NAG8-815 and DARA, the German Aeronautics and Space Agency. One of the authors would like to acknowledge the financial support provided by the Department of Defense in the form of a National Defense Science and Engineering Fellowship. One of the authors acknowledges very useful discussions with many members of the MIT community, especially Prof. Markus Zahn, Prof. Alar Toomre, Mr. Robert Hyers, and Ms. Livia Racz.

References

[1] I. Egry and J. Szekely, "The Measurement of Thermophysical Properties in Microgravity Using Electromagnetic Levitation," Adv. Space Res., 11(7)(1991), 263-266.

[2] E. Schwartz, J. Szekely, O.J. Ilegbusi, J-H. Zong, and I. Egry, "The Computation of the Electromagnetic Force Fields and Transport Phenomena in Levitated Metallic Droplets in the Microgravity Environment", MHD Symposium, 1992 TMS Meeting, San Diego, 81-87.

[3] N. El-Kaddah and J. Szekely, "The Electromagnetic Force Field, Fluid Flow Field, and Temperature Profiles in Levitated Metal Droplets", Metallurgical Transactions B, 14(1983), 401-410.

[4] J-H. Zong, J. Szekely, and E. Schwartz, "An Improved Computational Technique for Calculating Electromagnetic Forces and Power Absorptions Generated in Spherical and Deformed Body in Levitation Melting Devices", IEEE Transactions on Magnetics, 28(3)(1992), 1833-1842.

[5] R. Dudley and P.E. Burke, "The Prediction of Current Distribution in Induction Heating Installations", IEEE Transactions on Industry Applications, IA-8(5)(1972), 565-571.

[6] P.E. Burke, P.P. Biringer, P.F. Ryff, and E. Solger, "The Prediction and Measurement of Current Distribution in Coaxial Circular Geometries", 6th PICA Conference Proceedings (1969), 464-482.

[7] A.J. Mestel, "Magnetic Levitation of Liquid Metals", Journal of Fluid Mechanics, 117(1982), 27-43.

[8] A. Gagnoud, J. Etay, and M. Garnier, "The Levitation Melting Process Using Cold Crucible Technique", Transactions ISIJ, 28(1988), 36-40.

[9] D.W. Fugate and J.F. Hoburg, "Shape and Stability Comparisons of Electromagnetically Confined Liquid Metal Boundaries", Metallurgical Transactions B, 24(1993), 171-178.

[10] A.D. Sneyd and H.K. Moffatt, "Fluid Dynamical Aspects of the Levitation-Melting Process", Journal of Fluid Mechanics, 117(1982), 45-70.

[11] A. Gagnoud and M. Garnier, "Physical Analysis and Modelization of Phenomena in Electromagnetic Levitation in Conical Conductor", IEEE Transactions on Magnetics, 21(5)(1985), 1886-1888.

[12] A. Gagnoud and J.P. Brancher, "Modelling of Coupled Phenomena in Electromagnetic Levitation", IEEE Transactions on Magnetics, 21(6)(1985), 2424-2427.

[13] A. Gagnoud and I. Leclercq, "Free Boundary Problem in Electromagnetic Levitation Melting and Continuous Casting", IEEE Transactions on Magnetics, 24(1)(1988), 256-268.

[14] N. El-Kaddah and F.A. Acosta-Gonzalez, "Mathematical Model for the Shaping of Molten Metal by an Electromagnetic Field", Casting of Near Net Shape Products, Warrendale, PA, TMS, 1988, 423-437.

[15] N. El-Kaddah and T.T. Natarajan, "The Influence of Coil Design on Melt Shape in Electromagnetic Levitation Melting", Proceedings of the Sixth International Iron and Steel Congress, Nagoya, Japan, ISIJ, 1990, 380-387.

[16] J.R. Bhamidipati and N. El-Kaddah, "Calculation of Electromagnetic Field and Melt Shape in the Magnetic Suspension Melting Process", MHD Symposium, 1992 TMS Meeting, San Diego, 69-74.

[17] J. Melcher, Continuum Electromechanics, MIT Press, Cambridge, MA, 1981.

[18] D.N. Riahi and J.S. Walker, "Float Zone Shape and Stability with the Electromagnetic Body Force Due to a Radio-Frequency Coil", Journal of Crystal Growth, 94(1989), 635-642.

[19] B.Q. Li and J.W. Evans, "Computation of Shapes of Electromagnetically Supported Menisci in Electromagnetic Casters--Part I: Calculations in Two Dimensions", IEEE Transactions on Magnetics, 25(6)(1989), 4443-4448.

[20] T. Sato, S. Sugiyama, A. Yada, M. Nakada, K. Mori, and T. Osako, "Analytical and Experimental Investigation on Control of Molten Metal Surface in Continuous Casters under Magnetic Pressure", 1991 1st ASME-JSME Fluids Engineering Conference, Portland, Oregon.

[21] J.W. Evans, D.P. Cook, and S. Nishioka, "Mathematical and Physical Modeling of Electromagnetically Supported Melts in Three Dimensions", MHD Symposium, 1992 TMS Meeting, San Diego, 35-44.

[22] D.P. Cook, J.W. Evans, and J. Grandfield, "Application of a Mathematical Model in Thin Strip Electromagnetic Casting", MHD Symposium, 1992 TMS Meeting, San Diego, 145-149.

[23] P. Gerhart, R. Gross, and S. Hochstein, Fundamentals of Fluid Mechanics, Addison-Wesley Publishing Company, Reading, MA, 1992.

[24] L.M. Racz, J. Szekely, and K.A. Brakke, "A General Statement of the Problem and Description of a Proposed Method of Calculation for Some Meniscus Problems in Materials Processing", ISIJ International, 33(2)(1993).

[25] D.M. Herlach, R. Willnecker, and F. Gillessen, ESA SP-222 (1984), 399.

[26] I. Egry, "Surface Tension Measurements of Liquid Metals by the Oscillating Drop Technique", J. Mat. Science, 26(1991), 2997-3003.

[27] S. Sauerland, K. Eckler, and I. Egry, "High Precision Surface Tension Measurements on Levitated Aspherical Liquid Nickel Droplets by Digital Image Processing", Journal of Mat. Sci. Letters, 11(1992), 330.

[28] D.L. Cummings and D.A. Blackburn, "Oscillations of Magnetically Levitated Aspherical Droplets", J. Fluid Mech., 224(1991), 395.

[29] P.V.R. Suryanarayana and Y. Bayazitoglu, "Effect of Static Deformation and External Forces on the Oscillations of Levitated Droplets", Phys. Fluids A, 3(5)(1991), 967.

[30] H. Fukumoto, Y. Hosokawa, K. Ayata, and M. Morishita, "Numerical Simulation of Meniscus Shape Considering Internal Flow Effects", MHD Symposium, 1992 TMS Meeting, San Diego, 21-26.